Bilateral series resonant inverter for high frequency link UPS

Y.H. Chung, PhD
B.S. Shin, MSc
G.H. Cho, PhD

Indexing terms: Inverters, Power electronics

Abstract: A bilateral series resonant inverter for a high frequency link uninterruptible power supply is described. The proposed inverter consists of a zero current switched series resonant convertor, a high frequency transformer and a zero current switched cycloconvertor, where bidirectional power flow and high efficiency are obtained. In the proposed inverter, the output voltage is regulated by controlling the resonant tank energy. The switching pattern of the cycloconvertor is fixed to obtain the high frequency transformer. A new control scheme to minimise the output ripple voltage is suggested and verified through computer simulation and experiment, and the effects of the circuit parameters on the output voltage ripple are discussed.

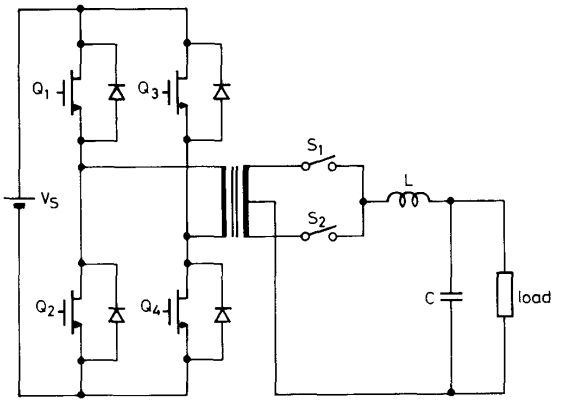

Fig. 1 *Power circuit of high frequency link UPS proceeded by DC/AC convertor for isolation*

1 Introduction

It is well known that demands for the uninterruptible power supply (UPS) have been rapidly increased. Many types of UPS have been developed for various applications. Among them, a small UPS less than 1 kW is interesting especially in microcomputers and other electronic devices concerning office and home automation. Small size and low cost are required for these applications of the UPS. To achieve such characteristics, it is necessary to minimise the output filter and the isolation transformer of UPS by using the high frequency link power conversion schemes [1–3].

Fig. 1 shows the case where the isolation is made in the high frequency inverter followed by the cycloconvertor. The high frequency inverter provides a pulse width modulated high frequency voltage through the high frequency transformer. After high frequency isolation, the cycloconvertor outputs a voltage whose frequency is the same as the commercial AC line frequency by appropriately converting the polarity of rectangular pulses. Even though the size of the UPS is small, the switching stresses of devices and the EMI noises become severe as the switching frequency increases. There is also a possibility of saturation of the isolation transformer.

Fig. 2 shows the case where the isolation is made in the series resonant convertor (SRC) followed by low frequency inverter. DC power is converted into a sinewave modulated high frequency waveform by controlling the phase difference between twin resonant circuits. The resultant AC waveform is then rectified by the high frequency diode bridge and filtered for suppression of the high frequency components. The resulting half sinusoidal waveform is inverted once every two half periods by a low frequency inverter. In this circuit, EMI noise is decreased by using a resonant circuit and the possibility of saturation of the isolation transformer is eliminated. The power flow of this method is unidirectional and it still has the switching stresses in the resonant circuit because the switching does not occur at zero voltage or zero current instant.

The SRC circuit is modified, as shown in Fig. 3, so that the output voltage of SRC can swing from the negative value to the positive value by replacing the diodes in the output rectifier with the bidirectional switches. If the modified SRC, called a series resonant inverter (SRI) is operated at constant resonant frequency, then the switching operations occur at zero current level. Even though the switching instants of the SRI are fixed at the current zero crossing points, it is possible to control the resonant tank energy by controlling the ratio of the powering

Paper 7997B (P6), first received 19th December 1989 and in revised form 26th June 1990

Y.H. Chung is with Goldstar Industrial Systems, Lucky-Goldstar Research and Development Complex, 533 Hogae-Dong, Anyang-Shi, Kyongki-Do, 430-080, Korea

B.S. Shin and G.H. Cho are with the Department of Electrical Engineering, Korea Advanced Institute of Science and Technology, PO Box 150, Cheong-Ryang, Seoul, Korea

interval to the regenerating interval. The bidirectional switches (S1 and S2) are in synchronisation with the current zero crossing points, so the problems of switching stresses and EMI noise can be solved. The basic operation of SRI is explained and a guide line determining the reactive elements is given. The proposed control scheme is verified through computer simulation and an experiment.

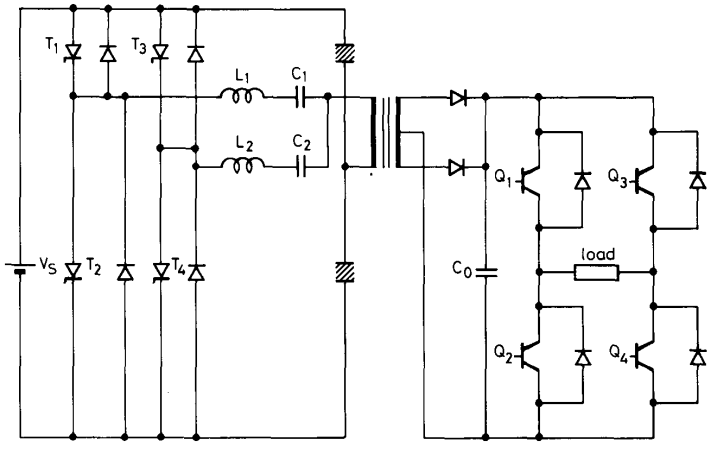

Fig. 2 *Power circuit of high frequency link UPS proceeded by resonant convertors for isolation*

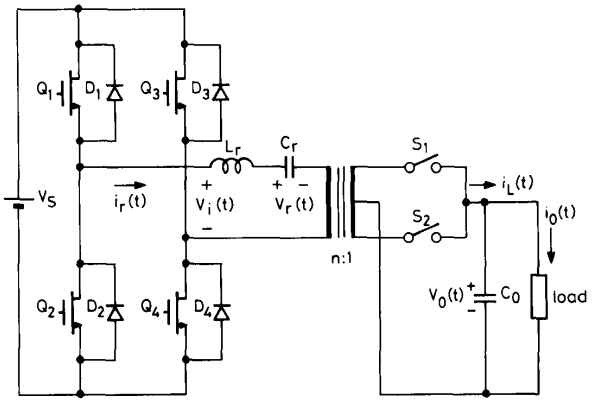

Fig. 3 *Power circuit of proposed series resonant inverter*

2 Operation of SRI

Fig. 3 shows the power circuit of SRI where it can be shown that only the rectifier diodes of SRC are replaced with the bidirectional switches (S1 and S2). The basic operation of the SRI is similar to the quantum series resonant convertor of Reference 5, except for the ability of the bidirectional power flow of SRI. Even though the half bridge SRC can be used in Fig. 3, the full bridge SRC is adopted because it requires the low current stresses of elements in the primary side of the isolation transformer and it is more flexible to control the resonant tank energy (RTE). In Fig. 3, the switch on/off always occurs in synchronisation with the current zero crossing points. In that case, there are three useful switch modes as shown in Fig. 4, which are called the powering mode, the free resonant mode and the regenerating mode. These modes are classified according to the direction of the power flow from the source side to the resonant tank side. As the SRI is bilateral, there are three additional switch modes if the load side is regarded as the power source. Because the operation seen from the load side is similar to that from the source side, only explanation from the source side is given. The description of each mode is as follows:

2.1 Powering mode

Switches Q1 and Q4 or Q2 and Q3 are turned on and off alternately, and two bidirectional switches, S1 and S2, are turned on/off in synchronisation with the resonant current zero crossing points. The inverter voltage, $V_i(t)$, and the resonant current, $i_r(t)$, are in phase as shown in Fig. 4*a*. During this mode, the source power is delivered to the L_r, C_r tank. The energy flow from the load side to the tank side may be positive or negative depending on the output capacitor voltage $V_0(t)$ and the bidirectional switch condition. This mode is used to rapidly increase the tank energy.

2.2 Free resonant mode

Switches D2 and Q4, and Q2 and D4, or equivalent D1 and Q3, and Q1 and D3 are turned on and off alternately, and two bidirectional switches, S1 and S2, are turned on/off in synchronisation with the resonant current zero crossing points. In this mode, the inverter voltage $V_i(t)$ is zero. The sinusoidal resonant current is gradually decreased or increased depending on the output conditions as shown in Fig. 4*b*.

2.3 Regenerating mode

When four switches, Q1–Q4, are turned off, diodes D1 and D4 or D2 and D3 are turned on and off alternately, and two bidirectional switches, S1 and S2, are turned on/off in synchronisation with the resonant current zero crossing points. During this mode, the inverter voltage $V_i(t)$ and the resonant current are out of phase as shown in Fig. 4*c*. The tank energy is recovered to the source side. The energy flow from the load side to the tank side may be positive or negative depending on the output capacitor voltage and the bidirectional switch condition. This mode is used to rapidly decrease the tank energy.

If the resonant link current is positive (negative) when the switch S1 is turned on, the output capacitor voltage is increased (decreased) rapidly or gradually depending on the corresponding resonant mode. Similar results are

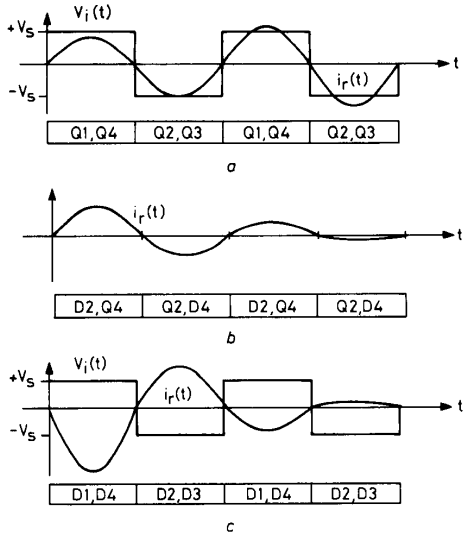

Fig. 4 *Typical waveforms of tank circuit for three modes*
a Powering mode
b Free resonant mode
c Regenerating mode

obtained when the switch S2 is turned on. Namely, the bidirectional switches S1 and S2 are operated as a cycloconvertor, appropriately distributing the resonant link current to the output capacitor and the load. It can be shown that there are several methods to control the output voltage. Assume that the resonant link current is controlled to be constant irrespective of the load condition and the output switching state. The output voltage of the SRI can be controlled by appropriately selecting one of two switches as shown in Fig. 5. If the output

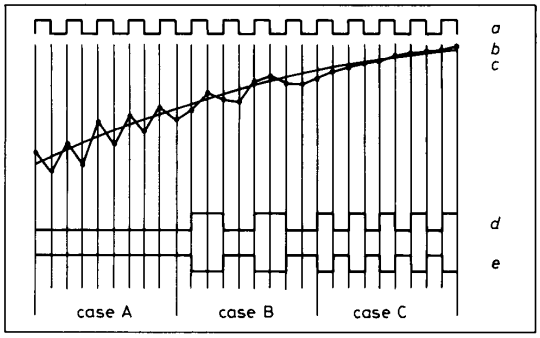

Fig. 5 *Output switching patterns for several cases*
a Polarity of the resonant link current
b Output voltage command
c Output voltage
d Turn-on interval of S1
e Turn-on interval of S2

voltage is greater than the reference voltage, one of two switches is turned on to decrease the output voltage, and vice versa.

In case A, shown in Fig. 5, the output voltage is corrected at every half resonant cycle, which is similar to the delta modulation of voltage source inverter. Even though the output voltage is well controlled in this case, the switching frequency of the isolation transformer is much lower than the resonant frequency because the voltage across the transformer is determined by the output voltage and the switching condition of S1 and S2. Only one of two switches is successively connected to the output capacitor, which is undesirable in reducing the size of the isolation transformer.

In case B, shown in Fig. 5, the output voltage is increased (decreased) during a half resonant interval and decreased (increased) during the next half resonant interval. If the increased quantity is greater (less) than the decreased one, then the resultant output voltage is increased (decreased). The output voltage is regulated by controlling the RTE during every half resonant interval. One of the two output switches is successively turned on during one resonant interval. In this case, the operating frequency of the transformer is one half of the resonant frequency.

In case C, shown in Fig. 5, the output voltage is successively increased to follow the reference voltage with some error without changing its slope. Because the output switches are alternately turned on and off at every half resonant period, the switching frequency of the transformer is the same as the resonant frequency. Similar results are obtained when the output voltage is successively decreased. If the resonant current changes its polarity at every half cycle, there are some problems when the slope of the output voltage is to be changed because there are no means to change it with the fixed output switching pattern. There are two possibilities to overcome such a problem. One of them is to allow the output switches to be turned on successively during one resonant interval only when the slope of the output voltage is to be changed. In this case if the effective link current $i_L(t)$ which is supplied to the output capacitor and the load is well regulated, to follow the required current, this approach is reasonable. However, if the load variation occurs frequently and discontinuously, e.g. rectifier load, this method is not satisfactory in reducing the size of the isolation transformer.

Another method is to change the polarity of the effective link current $i_L(t)$ as shown in Fig. 6 where the typical

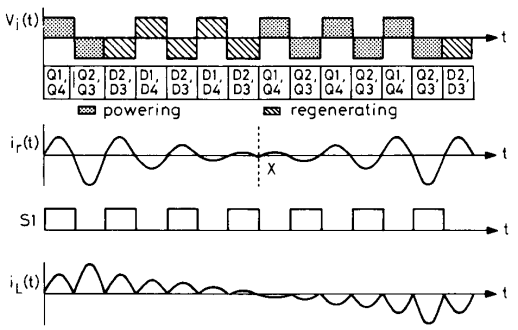

Fig. 6 *Typical waveforms with fixed output switching pattern*

waveforms are given with the fixed output switching pattern. If the polarity of $i_L(t)$ is to be changed, the resonant circuit is successively operated at the regenerating mode. Even though the turn-on signals are applied to the switches in parallel with the conducting diodes, the gated switches are not operated until the free wheeling diodes D1–D4 are reversely biased. The gated switches are conducting when the diodes are reversely biased marked X in Fig. 6. The polarity of the effective link current is changed from positive to negative with the fixed output

switching pattern. This method is most desirable in reducing the size of the isolation transformer and has thus been adopted.

From these considerations, the following results can be summarised:

(*a*) The switching pattern of the output switches should be fixed to minimise the isolation transformer.

(*b*) During a half resonant interval, transferred energy from the tank circuit (output capacitor) to the output capacitor (tank circuit) should be limited to minimise the output voltage ripple.

(*c*) As the output voltage ripple is dominantly dependent on the RTE for given reactive parameters (L_r, C_r, C_0), it is necessary to control the RTE according to the load condition.

(*d*) Because there is not enough time to determine the mode selection when the resonant current reaches zero, the proposed SRI requires an estimator to give the next switching states.

The mathematical modelling of the SRI is given and control schemes are discussed.

3 Modelling and output voltage control of SRI

Fig. 7 shows the equivalent circuit of the SRI where $M_1(t)$ and $M_2(t)$ represent the switching states of the resonant

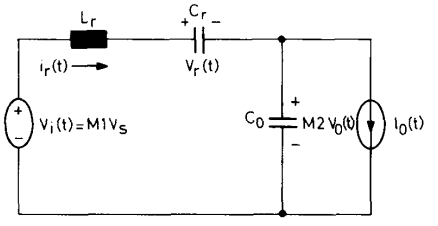

Fig. 7 *Equivalent circuit during resonant operation*

tank side and the output switch (S1, S2) side, respectively, and can be defined as

$$M_1(t) = \begin{cases} +1 & V_i(t) = +V_s \\ 0 & V_i(t) = 0 \\ -1 & V_i(t) = -V_s \end{cases}$$

$$M_2(t) = \begin{cases} +1 & \text{S1 is on} \\ -1 & \text{S2 is on} \end{cases}$$

The following relationships can be obtained from Fig. 7:

$$L_r \frac{di_r(t)}{dt} = -v_r(t) + M_1(t)V_s - nM_2(t)v_0(t) \quad (1)$$

$$C_r \frac{dv_r(t)}{dt} = i_r(t) \quad (2)$$

$$C_0 \frac{dv_0(t)}{dt} = nM_2(t)i_r(t) - i_0(t) \quad (3)$$

where n is turns-ratio of the isolation transformer.

Because the mode selections or the switching instants of switches S1 and S2 are only allowed when the resonant tank current crosses the zero point, the controls of the RTE and the output voltage can be obtained discretely. These characteristics mean that the SRI can be controlled digitally and modelled by the difference equations. Because the peak value of the tank capacitor voltage (inductor current) is related to the stored energy in the capacitor (inductor), and the tank capacitor voltage (inductor current) changes sinusoidally during the resonant interval, it is desirable to solve eqns. 1, 2 and 3 as functions of peak values of the tank variables. Let all peak variables be denoted by the index k and the capital letter during the kth half resonant period, as shown in Fig. 8. If the resonant frequency ω_r and the output capacitor C_0 are sufficiently greater than the output frequency ω_0 and the resonant capacitor C_r, respectively, then the output capacitor and the output load can be replaced by a constant voltage source and a constant current source, respectively, during a half resonant interval. In this case, the following results can be obtained from eqns. 1–3:

$$I_{r,k} = \frac{-V_{r,k} - nM_{2,k}V_{0,k} + M_{1,k}V_s}{Z_r} \quad (4)$$

$$V_{r,k+1} = -V_{r,k} - 2nM_{2,k}V_{0,k} + 2M_{1,k}V_s \quad (5)$$

$$V_{0,k+1} \approx V_{0,k} - n\delta_1 M_{2,k}V_{r,k} + \delta_1 M_{1,k}M_{2,k}V_s - \delta_2 I_{0,k} \quad (6)$$

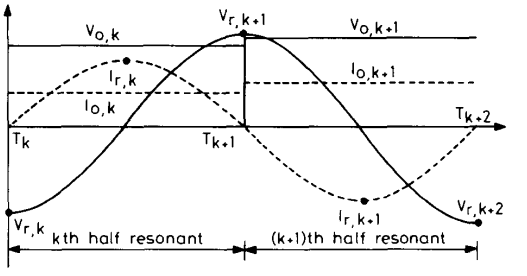

Fig. 8 *Definition of peak variables*

where, $\delta_1 = 2C_r/C_0$, $\delta_2 = \pi\sqrt{(L_r C_r)}/C_0$ and $Z_r = \sqrt{(L_r/C_r)}$.

Because the next switching state, $M_{2,k+1}$, of the output switches S1 and S2 is automatically determined by the present switching state, $M_{2,k}$, it is sufficient to know the next resonant tank mode, $M_{1,k+1}$. Eqn. 6 means that it is possible to predict the next output voltage $V_{0,k+1}$ if the present states are known, i.e., peak capacitor voltage, $V_{r,k}$, output voltage, $V_{0,k}$, load current, $I_{0,k}$, and switching states, $M_{1,k}$ and $M_{2,k}$. If the estimated output voltage, $\hat{V}_{0,k+1}$, and the output voltage command, $V^*_{0,k+1}$, are known for the next state, the expected error quantities ($\hat{E}_{0,k+1} = V^*_{0,k+1} - \hat{V}_{0,k+1}$) can be obtained before the next switching occurs. Similarly, the error quantities at $t = T_{k+2}$ can be estimated for the possible states of $\hat{M}_{1,k+1}$ as shown in Fig. 9. Because

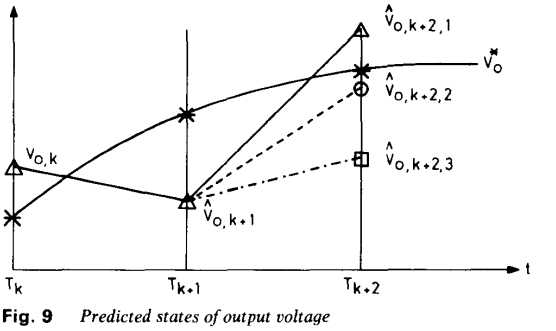

Fig. 9 *Predicted states of output voltage*

the state $\hat{E}_{0,k+2}$ can be estimated during the interval from $t = T_k$ to $t = T_{k+1}$, it is possible to determine the next optimum switching pattern for the minimum output voltage ripples.

The resonant current is measured to obtain the zero crossing point, so it is desirable to give the estimated output voltages ($\hat{V}_{0,k+1}$ at $t = T_{k+1}$, $\hat{V}_{0,k+2}$ at $t = T_{k+2}$) as a function of link current which can be written by using eqns. 4–6 as

$$\hat{V}_{0,k+1} \approx V_{0,k} + n\delta_3 M_{2,k} I_{r,k} - \delta_2 I_{0,k} \quad (7)$$

$$\hat{V}_{0,k+2} \approx V_{0,k} - M_{2,k+1}\,\Delta M_1 n\delta_1 V_s + \Delta M_2\, n\delta_3 I_{r,k} - 2\delta_2 I_{0,k} \quad (8)$$

$$\hat{E}_{0,k+2} = V^*_{0,k+2} - \hat{V}_{0,k+2} \quad (9)$$

where, $\delta_3 = Z_r \delta_1$, $\Delta M_1 = M_{1,k} - M_{1,k+1}$ and $\Delta M_2 = M_{2,k} - M_{2,k+1}$.

As eqns. 7 and 8 can be implemented by using an analogue adder, the sign changer and sample/holder (S/H), the required estimator can be easily obtained without using an analogue multiplier.

Fig. 10 shows the control block diagram of the proposed SRI, where the measured quantities are the output voltage, $V_{0,k}$, the load current, $I_{0,k}$, the resonant inductor current, $I_{r,k}$, and the DC source voltage, V_s. The oscillator of Fig. 10 is synchronised to the zero crossing points of the resonant link current. Its free running frequency is slightly lower than the two times that of the resonant frequency so that a stable clock pulse can be obtained when the resonant current does not change its polarity as marked X in Fig. 6. The oscillator free runs if the trigger signal is not sensed. The output voltage command, V^*_0, is delayed by one resonant interval to easily obtain the next state command.

During the interval from $t = T_k$ to $t = T_{k+1}$ as shown in Fig. 9, the estimated output voltage $\hat{V}_{0,k+2}$ at $t = T_{k+2}$ can be obtained using eqn. 8. The estimated error at $t = T_{k+2}$ can therefore be obtained for the given next resonant mode ($M_{1,k+1}$). It is possible to determine the next resonant mode to minimise the output voltage error by comparing the estimated error quantities. The following procedure explains the aforementioned control concept:

(*a*) Sample and hold $V_{0,k}$ and $I_{0,k}$ at $t = T_k$

(*b*) Obtain $I_{r,k}$ by using a rectifier and a peak detector

(*c*) Determine the next switching state of the bidirectional switches, S1 and S2

$$M_{2,k+1} = -M_{2,k}$$

(*d*) Obtain the estimated errors at $t = T_{k+2}$ for the possible three cases by using eqns. 8 and 9 and the results of steps *a–c*

$$\varepsilon_1 = |\hat{E}_{0,k+2}| \quad \text{when } \hat{M}_{1,k+1} = +1$$

$$\varepsilon_2 = |\hat{E}_{0,k+2}| \quad \text{when } \hat{M}_{1,k+1} = -1$$

$$\varepsilon_3 = |\hat{E}_{0,k+2}| \quad \text{when } \hat{M}_{1,k+1} = 0$$

Determine $\hat{M}_{1,k+1}$ corresponding to the minimum estimated error

(*e*) Check the possibility of the over current of the reactor, that is

$$I_{r,k} \geq I_{r,max} \Rightarrow M_{1,k+1} = -\text{SIGN}(I_{r,k})$$

$$I_{r,k} > I_{r,max} \Rightarrow M_{1,k+1} = \hat{M}_{1,k+1}$$

(*f*) Apply the corresponding turn on signals as

$M_{1,k+1} = +1 \Rightarrow$ Q1 and Q4

$M_{1,k+1} = -1 \Rightarrow$ Q2 and Q3

$M_{1,k+1} = 0 \Rightarrow$ Q1 and Q3 or Q2 and Q4

$M_{2,k+1} = +1 \Rightarrow$ S1

$M_{2,k+1} = -1 \Rightarrow$ S2

4 Simulation and experimental results

Computer simulations were made for the rated power of 1 kW and the rated output voltage of 100 V (RMS) with the DC input voltage of 100 V. Because the resonant tank energy is controlled by the voltage difference between the inverter voltage $V_i(t)$ and the output capacitor voltage $V_0(t)$, the resistance load becomes the worst case. That is, the forcing function of the resonant circuit becomes minimum when the load current is maximum. In this sense, resistance load is used in the simulation.

Fig. 11 shows the simulation results for the output capacitor voltage and the load current waveforms when the load is changed from the light load to the full load. It shows that there is a very small transient interval and a very fast response is obtained. Fig. 12 shows the effective link current and the load current waveform for the load transient. Fig. 12 indicates that the variation of the load current is rapidly compensated by the resonant link current. Fig. 13 also shows that the isolation transformer is operated at the resonant frequency.

Figs. 14 and 15 show the output voltage, load current and effective link current, under the rectifier load condition, from which it can be shown that the distortion of

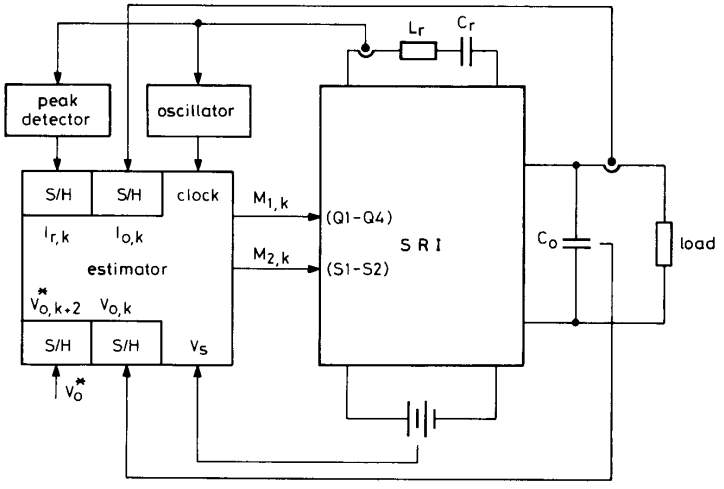

Fig. 10 *Control block diagram*

the output voltage is very low. This result comes from the configuration of the SRI and the adoption of high frequency link concepts. In the conventional inverter, the output voltage distortion is inevitable because a series

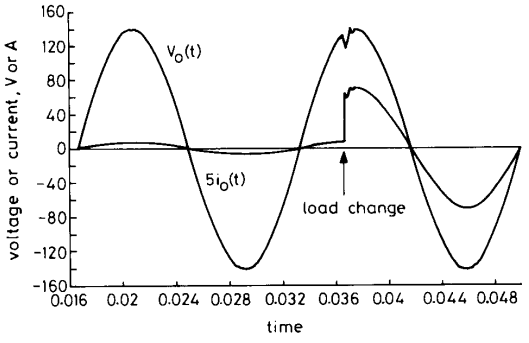

Fig. 11 *Output voltage and load current during load change*
Change from $R_0 = 100\ \Omega$ to $R_0 = 10\ \Omega$
$L_r = 173\ \mu H$; $C_r = 0.184\ \mu F$; $C_0 = 60\ \mu F$; $n = 0.5$

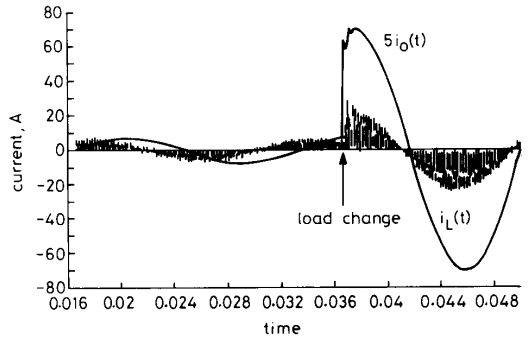

Fig. 12 *Effective link current and load current during load change*
Change from $R_0 = 100\ \Omega$ to $R_0 = 10\ \Omega$
$L_r = 173\ \mu H$; $C_r = 0.184\ \mu F$; $C_0 = 60\ \mu F$; $n = 0.5$

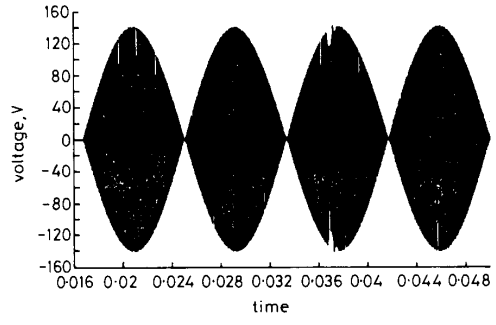

Fig. 13 *Isolation transformer voltage during load change*
Change from $R_0 = 100\ \Omega$ to $R_0 = 10\ \Omega$
$L_r = 173\ \mu H$; $C_r = 0.184\ \mu F$; $C_0 = 60\ \mu F$; $n = 0.5$

inductor is required in the output side for filtering [4]. The proposed SRI is operated in a similar manner to the current source inverter, and so only a parallel capacitor filter is adequate at the output side.

Fig. 16 shows the effects on the output voltage waveform when the turns-ratio of the isolation transformer is varied. If the turns-ratio n is increased, the difference voltage of the resonant tank circuit is decreased. This means that a minimum voltage difference across the tank circuit, which is dependent on the DC input voltage and the turns-ratio, is required to supply the required load current. Fig. 16 shows that the output voltage is seriously distorted when the turns-ratio is greater than 0.5.

Fig. 17 shows the total harmonic distortion (THD) factor for various output capacitance C_0, characteristic

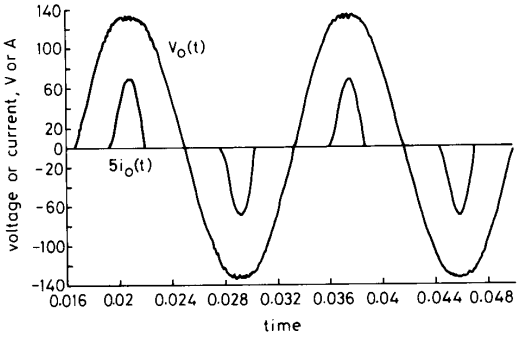

Fig. 14 *Output voltage and load current under rectifier load condition*
$L_r = 60\ \mu H$; $C_r = 1\ \mu F$; $C_0 = 100\ \mu F$; $L = 1$ mH; $C = 470\ \mu F$; $R = 100\ \Omega$; $n = 0.5$

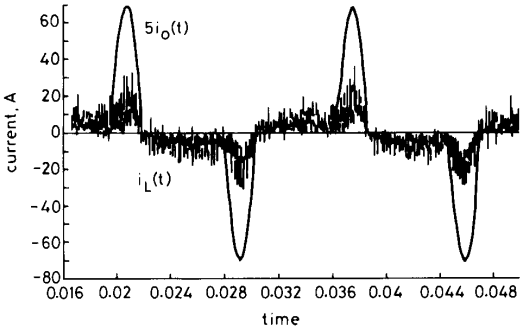

Fig. 15 *Effective link current and load current under rectifier load condition*
$L_r = 60\ \mu H$; $C_r = 1\ \mu F$; $C_0 = 100\ \mu F$; $L = 1$ mH; $C = 470\ \mu F$, $R = 100$; $n = 0.5$

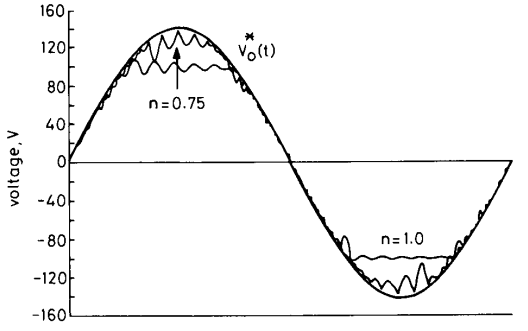

Fig. 16 *Effects on output voltages when the turn-ratio of transformer is varied*
$L_r = 60\ \mu H$; $C_r = 1\ \mu F$; $C_0 = 100\ \mu F$; $R_0 = 10$

impedance Z_r and the turns-ratio n. The THD decreases as the output capacitance and characteristic impedance increase. If the output capacitance increases, then the required reactive power also increases. Conduction loss increases under light load conditions. If the characteristic impedance increases, the voltage stress of the resonant capacitor increases. A compromise between the THD and the efficiency, or cost, is therefore required. Fig. 18 shows the frequency spectrum of the output voltage at the rated load condition and the switching frequency of 20 kHz. It shows that the harmonic components are greatly attenu-

ated. The most dominant harmonic is the resonant frequency component which is sufficiently lower than the fundamental component. In most applications, it is sufficient to add only a very small low pass filter at the output side.

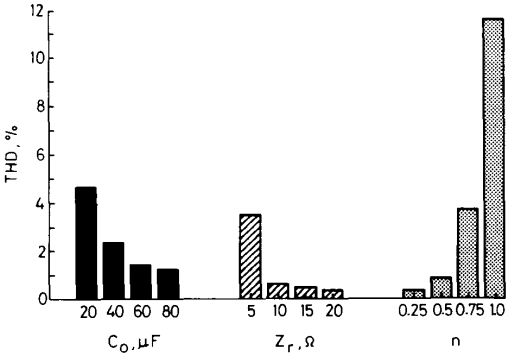

Fig. 17 *Total harmonic distortion factor for various output capacitance, characteristic impedance and turn ratio*

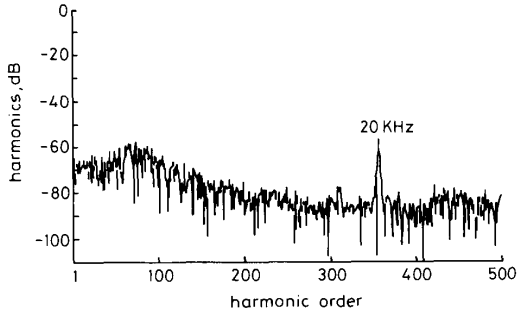

Fig. 18 *Frequency spectrum of output voltage*

Experimental results are given by Figs. 19–22. The switching frequency of this inverter is 28.2 kHz. Fig. 19

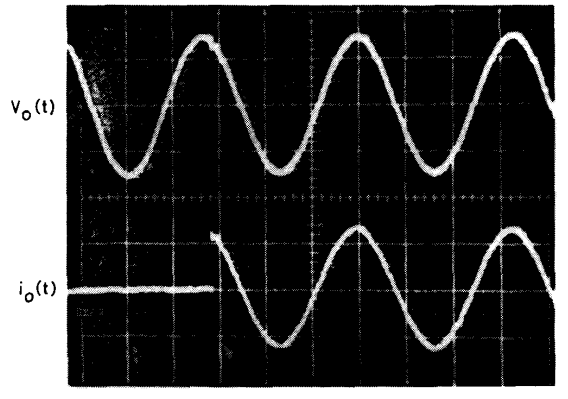

Fig. 19 *Oscillograms of output voltage and load current during load transient*
5 ms/div; 100 V/div; 10 A/div

shows the output voltage and the load current for the load transient case. It shows that there is a very small transient interval, and very fast response is obtained. Fig. 20 shows the load current and the effective link current for the load transient case where it can be shown that the variation of the load current is rapidly compensated by the resonant link current. Fig. 21 shows the output voltage when the load condition is varied periodically for several cycles. Fig. 22 shows the output voltage under rectifier load condition. It can be shown that the proposed inverter is well operated from these experimental and simulation results.

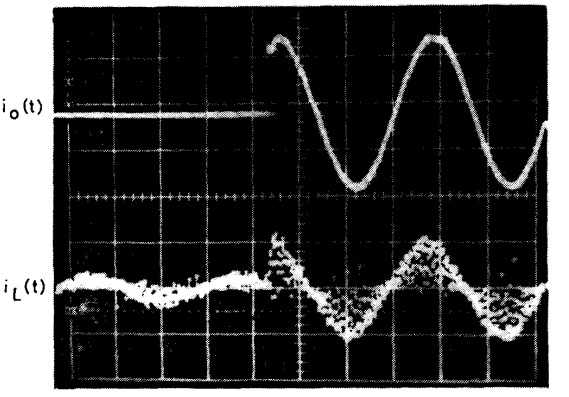

Fig. 20 *Oscillograms of load current and effective link current during load transient*
5 ms/div; 10 A/div; 20 A/div

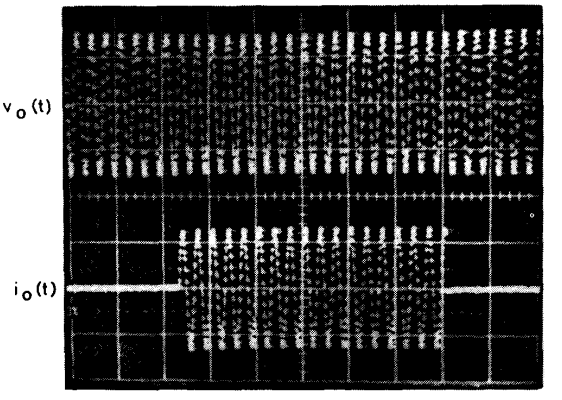

Fig. 21 *Oscillograms of output voltage and load current during periodical load variation*
50 ms/div; 100 V/div; 10 A/div

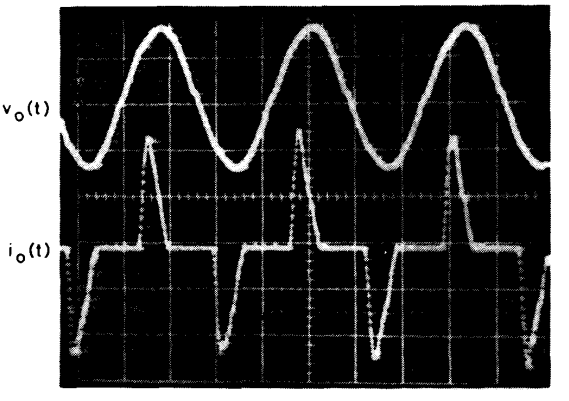

Fig. 22 *Oscillograms of output voltage and load current under rectifier load*
5 ms/div; 100 V/div; 5 A/div

5 Conclusions

A new power conversion system using a high frequency resonant link is proposed for the purpose of realising a compact, low acoustic noise, low EMI noise and high

performance UPS. A new control scheme to minimise the ouput voltage ripple is proposed and verified through computer simulation and experiment. The following conclusions can be obtained from the discussion presented in this paper:

(*a*) The proposed SRI is very simple and high efficient because of the zero current switching. The isolation transformer is minimised by the high frequency switching.

(*b*) Output voltage distortion is minimised by using the output voltage estimation control. The proposed control scheme is easily implemented by using an analogue circuit without using a high speed A/D convertor.

(*c*) Because the proposed inverter has no series inductor in the output filter side, it has very low voltage distortion in the rectifier load. The parallel operation of the proposed SRIs is very easy because of the configuration of the power circuit.

(*d*) A simple and compact UPS system can be realised by using this convertor.

6 References

1 MANIAS, S., ZIOGAS, P.O., and OLIVIER, G.: 'Bilateral DC to AC convertor using high frequency link', *IEE Proc.*, 1987, **134**, (1), pp. 15–23

2 HARADA, K., SAKAMOTO, H., and SHOYAMA, M.: 'Phase controlled DC-AC converter with high frequency switching'. IEEE PESC Conf. Record, Blacksburg, USA, 1987, pp. 13–19

3 YAMATO, I., TOKUNAGA, N., MATSUDA, Y., AMANO, H., and SUZUKI, Y.: 'New conversion system for UPS using high frequency link'. IEEE PESC Conf. Record, Tokyo, Japan, 1988, pp. 658–663

4 HANEYOSHI, T., KAWAMURA, A., and HOFT, R.G.: 'Waveform compensation of PWM inverter with cyclic fluctuating loads'. IEEE IAS Annual Meeting Conf. Record, Denver, USA, 1986, pp. 744–751

5 JEONG, G.B., and CHO, G.H.: 'Modeling of quantum series resonant converters — controlled by integral cycle mode'. IEEE IAS Annual Meeting Conf. Record, Pittsburgh, USA, 1988, pp. 575–582